Wind farms occupy fire-prone terrain but show no evidence of targeting burnt land: a multi-scale, time-ordered analysis for Greece

Stavros Stromatas

Independent Researcher · ORCID 0009-0005-9063-9282 · sstromts@gmail.com

This manuscript is a non-peer-reviewed preprint.

Abstract

A recurring claim in Greek public discourse holds that wildfires are set to clear land for wind farms, so that turbines end up on previously burnt ground. We test this claim with a design built to avoid the base-rate fallacy of simple overlap statistics, comparing the operational Greek wind fleet against wind-viable land with a use-availability case-control model and a time-ordered survival model, on a scale ladder from the parcel to 5 km. At the parcel scale there is no association, and thus no evidence of site-level targeting. At the landscape scale (2 to 5 km), when each wind farm is weighted equally, farms sit near burnt land with an odds ratio of about 1.6 compared with the wind-viable base rate; a fire-prone fuel covariate explains roughly half of this, leaving a residual near 1.4 that survives adjustment for terrain, fuel, and protected status. The landscape signal disappears when individual turbines rather than farms are the unit, because larger developments are less frequently adjacent to recorded burnt areas and dominate the turbine count. The time-ordered test is not robust, and the median fire-to-installation gap is 6 to 7 years. The evidence does not support deliberate burning to build; it does show that wind farms occupy fire-prone landscapes to a degree that measured landscape covariates only partly explain, most plausibly through unmeasured static co-location rather than a temporal fire-to-installation process.

Keywords: wind energy; wildfire; land use; use-availability; survival analysis; Greece

1. Introduction

The rapid expansion of onshore wind energy across fire-prone Mediterranean landscapes has been accompanied, in Greece, by a persistent public accusation: that wildfires are deliberately set to clear forest which would otherwise block development, so that wind turbines are subsequently installed on the burnt land. The claim recurs in Greek media, social media, and local opposition to specific projects, and it matters beyond Greece because similar suspicions attach to renewable-energy siting in many fire-prone regions. If the claim were true, it would imply that turbine locations coincide with previously burnt ground at a rate above what siting on wind grounds alone would produce, and that fire tends to precede installation in a way consistent with intent.

Testing such a claim rigorously is harder than it first appears, and the intuitive tests mislead in two distinct ways. First, turbines occupy very little ground, so any statistic of the form "turbine footprint as a fraction of burnt area" is tiny by construction and says nothing about preference; a vanishing ratio is fully compatible with strong selection, and a large ratio would be impossible regardless of behaviour. Second, and more fundamentally, the relevant comparison is not against all land, or against all burnt area, but against comparable wind-viable land. Greece burns extensively every year, and wind development concentrates on exposed ridgelines that are themselves dry, wind-swept, and fire-prone. A raw spatial overlap between turbines and burnt areas is therefore expected even under entirely innocent siting. Establishing preference requires a base rate defined on the land where turbines could plausibly be placed, and establishing the causal direction implied by the accusation requires ordering fire against installation in time.

Asking whether a set of chosen locations is drawn preferentially from an available landscape is the use-availability problem of habitat and resource-selection analysis in ecology (Johnson, 1980; Manly et al., 2002; Boyce et al., 2002), in which "used" points are contrasted with a random sample of "available" background under covariate adjustment. Framing that contrast as cases against controls sampled from an eligible universe is the logic of spatial epidemiology (Elliott & Wartenberg, 2004). Separating genuine siting preference from landscape confounding, finally, is a recurring difficulty in studies of where energy and other infrastructure is built (Diffendorfer & Compton, 2014). The methods deployed here are therefore not specific to Greece; they transfer to any contested siting claim for which a defensible set of available locations and a credible time ordering can be constructed.

The only prior public analysis of this specific Greek claim that we are aware of is a conference poster by the Hellenic Wind Energy Association (Vlamakis et al., 2025). It reports that wind farms occupy at most 0.07% of legally reforestable land, and that turbines installed after a fire cover 0.03% of the area burnt over the period 2008 to 2024, and it concludes that there is no correlation. Those figures are footprint-over-area ratios, small by construction, computed over reforestable or burnt land rather than over wind-viable land, and they carry no inferential test of preference or of time ordering. They can motivate the question but cannot resolve it, and, as we show, a landscape-scale association does in fact exist once an appropriate base rate is used.

Our central result is more nuanced than a clean null. We find no evidence of parcel-level targeting and no evidence of deliberate burning to build. We do, however, find a robust landscape-scale association between wind farms and burnt land that our measured covariates only partly explain, and we are careful throughout to distinguish that residual spatial association from the causal claim the accusation actually makes. The paper's contribution is thus twofold: a substantive, evidence-based answer to a charged public question about Greek wind energy, and a methodological demonstration that the answer depends sharply on the unit of analysis, the spatial scale, and the completeness of the landscape controls.

2. Study area and data

The study covers the whole of Greece, a country with strong onshore wind resources on its mainland ridges and Aegean islands and with one of the highest wildfire burdens in the European Union. Wind development and wildfire both concentrate in dry, elevated, sparsely built terrain, which is precisely why a naive spatial overlap is uninformative and a base-rate design is required. Greece experiences hundreds of vegetation fires each year, and its largest seasons burn well over one hundred thousand hectares, with the burnt area concentrated in the same dry summers and exposed upland terrain that make ridgelines attractive for wind development. Onshore wind capacity has grown rapidly over the study period as part of national decarbonisation targets, and much of that growth has occurred on precisely the sparsely populated highland sites where fire is also most frequent. This shared geography is the source of the confounding that the present design is built to address, and it is the reason the question cannot be settled by inspecting a map of overlaps.

The unit of the wind fleet is the operational Greek Wind Power Station listed in the production-licence registry of the Regulatory Authority for Waste, Energy and Water (RAAEY), restricted to stations holding an operating licence (437 stations). Turbine geometry is taken from OpenStreetMap, which for Greek wind turbines matches the industry count closely; of 2,995 mapped turbines, 2,958 are assigned to a station within 5 km and 37 are orphans. The 437 operational stations are the subset, of a larger fleet of 508 licensed stations reported by industry, that carry an operating rather than merely a production or installation licence; the remainder are excluded because they are not yet operational or lack the licence status from which a commissioning date can be derived. The 37 orphan turbines, more than 5 km from any station, are excluded from all farm-level analyses and never enter any of the three tests. Commissioning dates were resolved from public administrative acts to exact dates (from the Di'avgeia transparency portal; 102 stations), to bounded intervals (113 stations), or to broader brackets from grid-operator records (117 stations); 105 stations remained unresolved, most of them either commissioned before 2008 or located on non-interconnected islands.

Fire perimeters come from the Copernicus European Forest Fire Information System (EFFIS) MODIS burnt-area product, which maps fires above a nominal 30 ha threshold as dated polygons. The public layer covers approximately 2016 onward; perimeters for 2010 to 2015 were obtained through the EFFIS data-request service within the same product family. The merged 2010 to 2024 dataset comprises 1,644 perimeters totalling 607,003 ha, consistent with the 615,363 ha reported for 2008 to 2024 by Vlamakis et al. (2025) once the two additional early years are allowed for.

Covariates are drawn from open products. Mean wind speed at 100 m is from the Global Wind Atlas; slope and aspect are derived from the Copernicus GLO-90 digital elevation model; land cover, including the fire-prone fuel classes used later, is from CORINE 2018; and protected status is from the Natura 2000 network. All raster operations are performed on a common 100 m grid in the ETRS89 Lambert Azimuthal Equal-Area projection (EPSG:3035). Table 1 summarises the sources and their roles.

Table 1. Data sources and their roles in the analysis.

Layer	Product	Native resolution	Role
Turbines	RAAEY licences and OpenStreetMap	point	cases and events
Fire	EFFIS MODIS burnt areas, 2010 to 2024	~250 m	exposure
Wind	Global Wind Atlas, 100 m mean speed	~250 m	universe gate and covariate
Elevation	Copernicus GLO-90	~90 m	slope and aspect covariates
Land cover	CORINE 2018	100 m	exclusions and fuel covariate
Protected areas	Natura 2000	vector	covariate

Source: compiled by the author.

3. Methods

Our design combines three complementary tests, each addressing a different facet of the accusation and each evaluated against the same eligible universe of wind-viable land. Test A asks, descriptively, whether fires tend to predate installation; it frames the ordering question but has no base rate. Test B asks whether wind farms are associated with burnt land more strongly than comparable wind-viable land would predict, using a use-availability case-control model; it is the core test of spatial preference. Test C asks whether a prior fire raises the subsequent probability of installation on eligible land, using a time-varying survival model in which fire enters as a time-dependent covariate; it is the core test of temporal direction. No single test is decisive alone: a spatial association without a time ordering points to shared static geography, whereas a genuine burn-to-build process should leave both a spatial signal and a positive, temporally ordered one. We therefore report all three across a common scale ladder and interrogate each for landscape confounding. The remainder of this section defines the eligible universe and then each test in turn.

3.1 The eligible universe

The eligible universe is the set of wind-viable land cells that serves as the denominator for all base-rate comparisons; it is the “available” set against which used locations are contrasted. Both defining thresholds are calibrated to the existing fleet. The wind floor is set to the fifth percentile of Global Wind Atlas speed at existing turbines, 5.96 m/s, close to the conventional 6.0 m/s cut-off, and the slope ceiling is set to the ninety-fifth percentile of slope at existing turbines, 16.07 degrees. We further exclude open water, glaciers, and dense artificial surfaces (CORINE classes 511 to 523, 335, 111, 112, 123, 124, and 141), and we mask to Greek land defined as the intersection of Global Wind Atlas validity and CORINE data presence. The resulting primary universe covers 17,361 km2, and 89.5% of turbines fall inside it, as expected under fleet calibration. Calibrating the universe to the fleet introduces a mild circularity, since cases help define the available set; we probe its consequences directly with a wind-by-slope threshold grid described below. Figure 1 shows the study area, the eligible universe, the burnt-area perimeters, and the turbine locations.

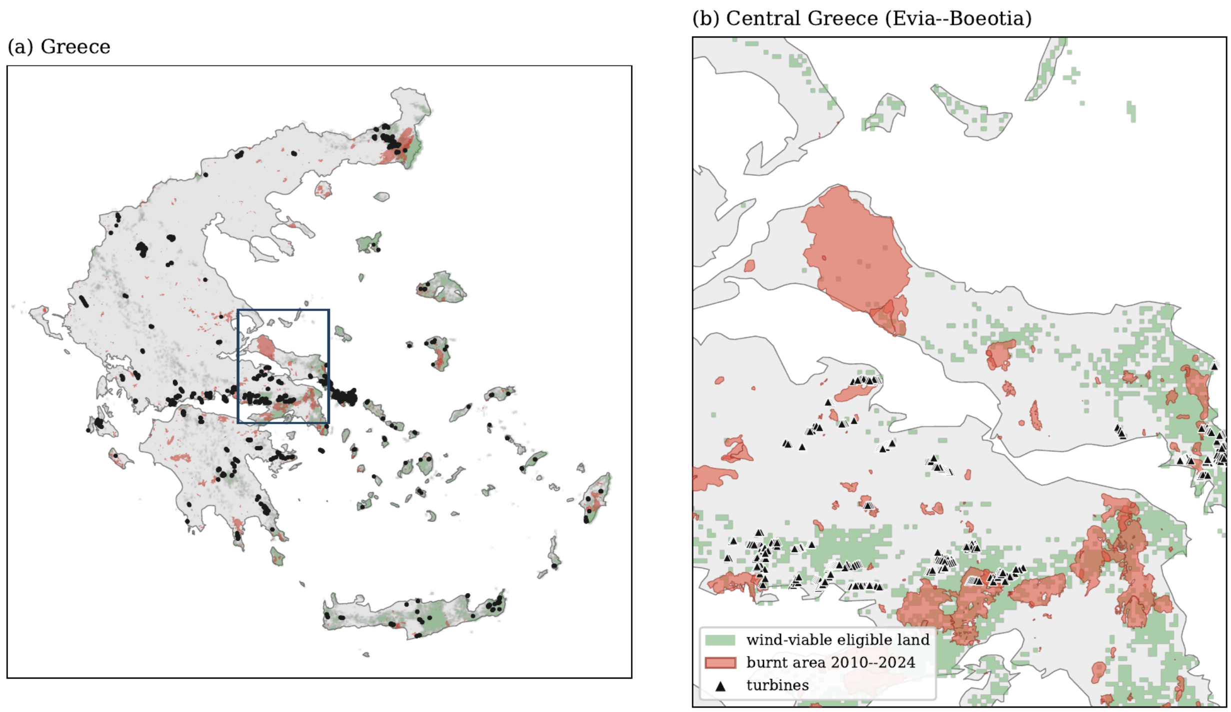

Figure 1: **Figure 1.** Study area. (a) Greece: national territory, wind-viable eligible land (green), burnt-area perimeters for 2010 to 2024 (red), and operational turbines (dark points); the box marks the inset. (b) Central Greece (Evia and Boeotia), showing turbines, burns, and eligible land within fire-prone terrain.

3.2 Test A: temporal precedence

For each station we form the convex hull of its turbines and buffer it at radii from 500 m to 5 km, then compare the dates of intersecting fires to the station’s commissioning window, classifying each station as having a fire that predates installation, that is ambiguous, that postdates installation, or none. Test A is purely descriptive and has no base rate; it is reported to show why raw counts, which grow with catchment size for every category simultaneously, cannot settle the question.

3.3 Test B: use-availability case-control

Controls are 30,000 cells drawn uniformly at random, without replacement, from the eligible universe, one point per cell, unweighted and unmatched; the count is a practical choice, and estimates are stable to it. The exposure is being burnt within the observation window, defined as a case or control point lying within a radius S of any 2010 to 2024 perimeter. We report two case definitions, because they answer materially different questions. In the turbine unit, cases are the 2,680 turbines inside the universe, with standard errors clustered by station to absorb within-farm correlation; because it weights each farm by its turbine count, this unit estimates the probability that an installed turbine lies near burnt land, and it is dominated by large developments. In the farm unit, cases are the 292 station centroids inside the universe, weighting each project equally; this unit estimates the probability that a wind-farm project is sited near burnt land. Both specifications are logistic regressions of case status on the burnt indicator plus wind speed, slope, elevation, aspect (represented as northness and eastness), and Natura status, with continuous covariates standardised. For multi-turbine farms the catchment is taken from the representative farm point. Test B counts any overlap within the window, including fires that postdate installation; the temporal direction is deferred to Test C.

3.4 Test C: time-varying survival

We follow eligible locations from 1 January 2010. The event is installation, meaning farm commissioning between 2010 and 2024 for stations with a resolvable date, and the risk set is a random sample of the eligible universe, administratively censored at 31 December 2024. All units enter at the time origin; there is no delayed entry or left-truncation. Stations installed before 2010, and stations with unresolved dates, are prevalent rather than incident and are excluded from the event set. The number of incident events is 165 when events are restricted to the eligible universe, our primary specification; when all resolvable farms are admitted, a sensitivity analysis, the number is 229. Fire enters as a time-dependent covariate that switches from zero to one at the fire date, so that only fires preceding a given time contribute to the hazard and post-installation fires never count. Events and controls are treated symmetrically as points sharing the same catchment. Following standard practice for the Cox model (Cox, 1972), we test the proportional-hazards assumption for the burnt effect using an interaction between the burnt indicator and follow-up time.

3.5 Scale ladder, fuel covariate, and robustness

Tests B and C are evaluated at radii from the point to 5 km, with the same radius applied to cases and controls so that the base rate moves with scale. To separate landscape fire-proneness from targeting, we add a scale-matched fuel covariate: the fraction of fire-prone natural fuel within the catchment, computed from CORINE forest, shrub, sclerophyllous vegetation, natural grassland, transitional woodland-shrub, and sparsely vegetated classes, and computed independently of where fire actually occurred. For the headline farm-level residual we replace seed-to-seed anecdote with a permutation test using 1,000 label permutations, and with a wind-by-slope threshold grid that rebuilds the eligible universe under nine combinations of wind floor and slope ceiling. In the gap analysis a short gap is defined as installation within three years of the fire.

3.6 Software, reproducibility, and use of AI tools

Analyses were implemented in Python using geopandas and rasterio for geospatial processing, statsmodels for the logistic models (Seabold & Perktold, 2010), lifelines for the time-varying Cox model (Davidson-Pilon, 2019), and scikit-learn for the permutation inference. All derived datasets and the full analysis code are openly archived (see Data availability). In line with the journal's policy on artificial intelligence, we disclose that an AI assistant was used to support parts of the research process, specifically the drafting and debugging of analysis code, language editing of the manuscript, and preparation of figures. All study-design decisions, statistical specifications, verification of numerical results, and final interpretations were made and checked by the author, who takes full responsibility for the content; AI tools were not used to generate or fabricate data and are not credited as authors.

4. Results

4.1 Temporal precedence

Burnt-before farm counts grow with catchment size, from 17 at 500 m to 95 at 5 km, but so do fires of every other category (Table 2); by 5 km almost every farm, and almost every random point, has a fire within range. A raw count therefore cannot distinguish preference from the background fire rate, which is exactly the base-rate problem the remaining tests are designed to overcome.

Table 2. Test A, farm-level temporal precedence for 302 resolved stations; 96 unresolved stations are reported separately.

Catchment	Predates	Ambiguous	Postdates	No fire
hull + 500 m	17	9	41	235
hull + 1 km	31	12	47	212
hull + 2 km	55	19	67	161
hull + 3 km	71	21	78	132
hull + 5 km	95	28	88	91

Source: authors' analysis of EFFIS and RAAEY data.

4.2 Spatial association depends on the unit

The spatial result hinges on whether farms are weighted equally or by their turbine count (Table 3, Figure 2). Under the turbine unit, the burnt association is null at every scale and is entirely removed by the fuel covariate. Under the farm unit, a strong and significant landscape-scale association emerges: the burnt odds ratio is 1.64 at 2 km, rising to 1.69 at 5 km. Adding the fuel covariate explains about half of this association but leaves a residual odds ratio of 1.40 at 2 km, 1.39 at 3 km, and 1.35 at 5 km, all statistically significant; at 1 km the fuel covariate removes the association entirely. The parcel scale is null in both units.

Table 3. Test B burnt odds ratio with 95% confidence intervals, unadjusted and with the fuel covariate, by unit and scale.

Scale	Turbine, unadjusted	Turbine, + fuel	Farm, unadjusted	Farm, + fuel
point	0.96 (0.62–1.47)	1.05 (0.69–1.61)	0.82 (0.50–1.33)	0.76 (0.47–1.24)
1 km	1.08 (0.82–1.41)	0.89 (0.67–1.18)	1.36 (1.03–1.79)	1.14 (0.86–1.50)
2 km	1.24 (0.97–1.58)	1.03 (0.80–1.33)	1.64 (1.28–2.10)	1.40 (1.09–1.80)
3 km	1.27 (0.99–1.64)	1.03 (0.79–1.35)	1.67 (1.30–2.14)	1.39 (1.08–1.78)
5 km	1.27 (0.95–1.70)	1.05 (0.76–1.44)	1.69 (1.29–2.21)	1.35 (1.02–1.78)

Source: authors' analysis.

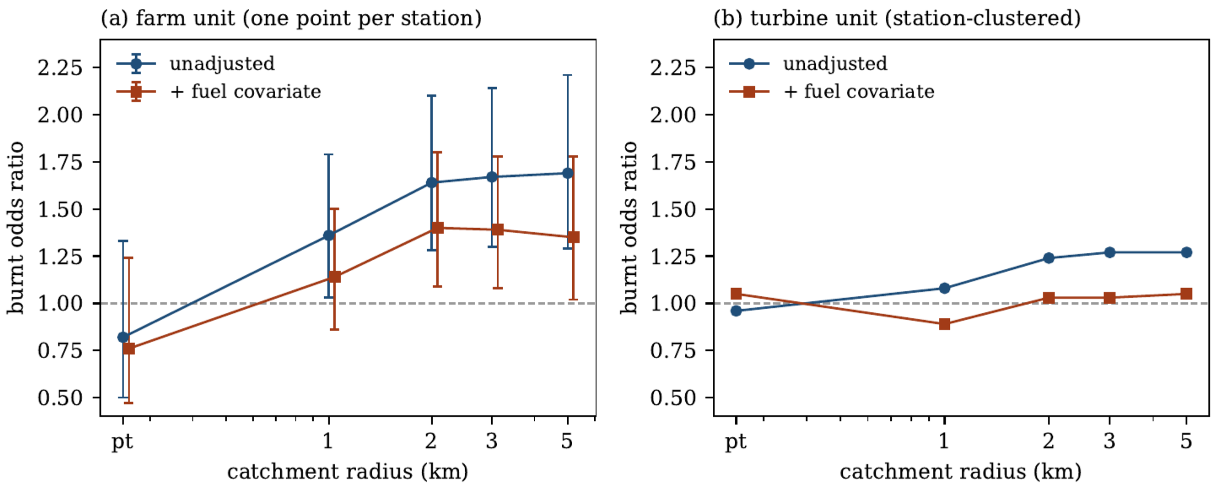

Figure 2: **Figure 2.** Test B burnt odds ratio with 95% confidence intervals, unadjusted and with the fuel covariate, across catchment radius. (a) Farm unit: a significant 2 to 5 km association with a residual near 1.4 after fuel. (b) Turbine unit: null and fully absorbed by fuel. The dashed line marks no effect.

The farm-level residual is robust to inference and to the definition of the universe. A permutation test on the 2 km fuel-adjusted estimate, using 1,000 label permutations, yields p = 0.010: the observed standardised burnt coefficient of 0.160 lies far outside the permutation null, which has a mean of approximately zero and a standard deviation of 0.061, roughly 2.6 standard deviations above it. Across the wind-by-slope threshold grid (Table 4), the fuel-adjusted odds ratio ranges from 1.26 to 1.47 and is significant in eight of the nine universe definitions, the sole exception being the loosest combination of wind and slope, at p = 0.052. The corresponding eligible areas and case counts are given in Table 5, confirming that the residual is not an artefact of a single universe size.

Table 4. Farm-level Test B at 2 km, fuel-adjusted burnt odds ratio with 95% confidence intervals, across eligible-universe thresholds.

	slope ≤ 15°	slope ≤ 18°	slope ≤ 20°
wind ≥ 5.5	1.39 (1.08–1.79)	1.33 (1.05–1.68)	1.26 (1.00–1.58)
wind ≥ 6.0	1.42 (1.10–1.83)	1.35 (1.06–1.72)	1.28 (1.01–1.62)
wind ≥ 6.5	1.47 (1.14–1.91)	1.38 (1.07–1.77)	1.32 (1.04–1.69)

Source: authors' analysis.

Table 5. Eligible-universe area (km2) and number of farm cases for each threshold in Table 4.

	slope ≤ 15°	slope ≤ 18°	slope ≤ 20°
wind ≥ 5.5	21,524 (n = 295)	25,199 (n = 326)	27,291 (n = 345)
wind ≥ 6.0	15,885 (n = 281)	18,726 (n = 311)	20,344 (n = 329)
wind ≥ 6.5	11,608 (n = 265)	13,782 (n = 291)	15,023 (n = 307)

Source: authors' analysis.

4.3 The time-ordered test is not robust

Treating events and controls symmetrically as points, the hazard ratio for prior burn is null when all 229 resolvable farms are admitted (2 km hazard ratio 1.12, 95% confidence interval 0.93 to 1.35, $p = 0.22$), but significant when events are restricted to the eligible universe (165 events; 2 km hazard ratio 1.32, $p = 0.007$; 3 km hazard ratio 1.25, $p = 0.017$). The fuel covariate leaves either version essentially unchanged. In the significant specification the proportional-hazards assumption is violated: the interaction between the burnt indicator and follow-up time is strong and negative ($p < 0.001$), so the effect is not constant over follow-up and the single hazard ratio is only a time-average. Because the estimate swings from null to significant across defensible design choices, and is non-proportional where it is positive, Test C does not provide robust evidence on the temporal direction in either direction.

4.4 Fire-to-installation gap

For farms that burnt before installation, the interval between fire and installation is long, with a median of 6 to 7 years, dominated by the five-to-ten-year bin and extending to 12 years (Table 6, Figure 3). Nearly every fire falls after the production licence, 30 of 32 at the 1 km catchment, which superficially matches the ordering the accusation implies but is mechanically forced: Greek licences were mostly issued before the fire record begins in 2010, so any incidental fire in the long licence-to-installation window necessarily lands after the licence. The genuinely suspicious profile, a short gap combined with a fire after the licence, appears in only 3 to 11 farms, consistent with chance given the roughly 10,000 vegetation fires of all sizes reported annually in Greece; the EFFIS perimeters used here, mapping fires above about 30 ha, number roughly 110 per year.

Table 6. Fire-to-installation gap and licence ordering for burnt-before farms; a short gap is installation within three years of the fire.

Catchment	n	Median gap (yr)	Fire after / before licence	Short gap and post-licence
hull	12	6.8	11 / 0	3
500 m	20	6.8	19 / 0	4
1 km	35	6.1	30 / 2	11

Source: authors' analysis.

5. Discussion

The parcel scale is null in every test, so there is no evidence that specific burnt parcels were selected for specific turbines. What survives is a landscape-scale spatial association, and its character can now be described precisely.

5.1 Why the unit of analysis matters

Whether the association appears at all depends on the analysis unit, and the reason is concrete rather than a statistical artefact. Larger farms are less fire-adjacent: the share of farms with a fire within 2 km falls from 0.50 in the smallest size tercile, with a median of two turbines, to 0.34 in the largest, with a median of twelve turbines, and burnt-proximity declines with farm size at an odds ratio of 0.57 per tenfold increase in turbine count ($p = 0.056$). Because the turbine unit weights each farm by its turbine count, these large, less fire-adjacent developments dominate it, and reweighting the farm model by turbine count reproduces the

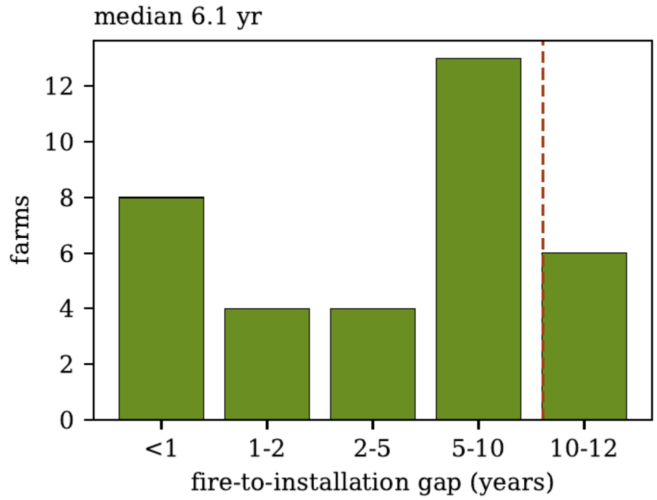

Figure 3: **Figure 3.** Fire-to-installation gap for burnt-before farms (1 km catchment, n = 35); median 6.1 years.

turbine-level estimate of about 1.22. The pattern is consistent with large developments concentrating in established, less fire-prone wind corridors while smaller projects disperse into fire-prone mountain terrain. Weighting each project equally, which is the natural way to think about a siting decision made once per project, yields the strong association of about 1.6 that fuel only half explains. This unit dependence is not a nuisance to be averaged away; it is itself a finding, and one that studies of infrastructure siting should confront explicitly, because turbine-weighted and project-weighted analyses of the same fleet can point in opposite directions.

5.2 What the residual means, and what it does not

We are deliberately cautious about interpreting the residual. It is robust to permutation and to threshold choices, which makes it unlikely to be a sampling artefact, and it shows that wind farms occupy fire-prone landscapes at the 2 to 5 km scale beyond what wind, slope, elevation, aspect, protected status, and fuel composition explain. Fuel, however, is only one landscape confounder. Road and grid access, land ownership and availability, planning and military exclusions, terrain roughness, and geology are all unmeasured here, and any of them could co-locate wind development with fire-proneness without any behavioural link between the two. The analyses cannot distinguish development that preferentially selects land already cleared by unrelated fires from residual spatial confounding by unmeasured siting factors; and neither of those possibilities is the same as deliberately burning land in order to build on it. For that deliberate-burning claim specifically, the evidence is unsupportive on every axis that bears on it: the parcel scale is null, the time-ordered hazard is fragile and non-proportional where positive, and the fire-to-installation gaps are long. A mechanism in which fires were intentionally set to facilitate construction would more naturally produce shorter and more consistent fire-to-installation intervals together with a stable positive temporal association; we observe neither.

5.3 Relation to prior work

These results both sharpen and qualify the flat “no correlation” conclusion of the industry poster (Vlamakis et al., 2025). A landscape-scale correlation does exist, and it is only partly explained by the covariates we measured, so a bare denial of any correlation is not supported by a base-rate analysis. At the same time, the correlation is not evidence for the accusation, which is specifically about burning land in order to build on it, and for that the site-level nulls, the fragile and non-proportional time ordering, and the long gaps are all unsupportive. The disagreement between the two studies is instructive: it stems entirely from the choice of denominator and from the presence or absence of a time-ordered test, which is precisely the methodological point of this paper.

5.4 Limitations

Several limitations qualify the findings. CORINE is a single 2018 snapshot, and for fires occurring before 2018 it already reflects post-fire land cover, so the fuel covariate carries measurement error and probably under-adjusts; the true landscape-explained fraction may be larger than half, which would shrink the residual. The MODIS-based EFFIS product maps only fires above about 30 ha, so small fires are absent. Commissioning dates for bracketed stations use interval midpoints, and the incident-event set for Test C is small, between 165 and 229, so the time-ordered test has limited power and, as shown, limited robustness. Test B counts any within-window overlap, including post-installation fires, which is appropriate for a spatial-association question but not for a temporal one, and is the reason the temporal question is handled separately by Test C. A further caveat concerns the definition of exposure. Because the farm-level catchment is measured from a representative point rather than from the full extent of each development, very large farms spread along a ridge may have their true fire exposure understated or overstated relative to compact ones; we retain the point-based definition for comparability with the point-based control sample, but note that alternative farm-extent definitions could shift the magnitude, though not the direction, of the landscape association. Finally, the analysis speaks to the systematic pattern across the fleet, not to any individual project, which it can neither implicate nor exonerate.

5.5 A methodological lesson

Beyond the Greek case, the study offers a transferable caution. The answer to "are these locations preferentially on land of type X" depends jointly on the unit of analysis, the spatial scale at which exposure is measured, and the completeness of the landscape controls, and moving any of the three can turn a null into a significant effect or the reverse. Honest treatment of all three, rather than the selection of whichever combination yields the cleanest message, is what separates a defensible finding from an artefact. The base-rate and time-ordered framework used here is portable to other contested siting claims in fire-prone regions and elsewhere.

6. Conclusions

Across temporal-precedence, spatial case-control, and time-ordered survival tests, evaluated from the parcel to 5 km and interrogated for landscape confounding and time gaps, we find no evidence that wind turbines in Greece are deliberately sited on burnt land: the parcel scale is null, the time ordering is fragile and non-proportional, and fire-to-installation gaps are long. We do find, robustly, that wind farms occupy fire-prone landscapes at the 2 to 5 km scale beyond what measured terrain, protection, and fuel explain, a residual most plausibly attributable to unmeasured static co-location factors rather than to any fire-to-installation process. We also find that this association is scale-of-development dependent: larger farms are less often adjacent to burnt land than smaller ones, so whether one counts projects or turbines changes the apparent result. The main practical lesson is methodological, and it applies wherever siting is contested: the answer depends on the analysis unit, the catchment scale, and the completeness of the landscape controls, and all three deserve to be reported openly.

Data availability

The derived datasets, including the merged fire perimeters, the eligible-universe raster, the terrain and land-cover layers, and the case-control and per-farm tables, together with the full analysis code, are openly archived on Zenodo (https://doi.org/10.5281/zenodo.21261873). Input products are third-party and used under their own licences: the RAAEY registry, OpenStreetMap, Copernicus EFFIS, the Global Wind Atlas, the Copernicus GLO-90 digital elevation model, CORINE, and Natura 2000.

References

Boyce, M. S., Vernier, P. R., Nielsen, S. E., & Schmiegelow, F. K. A. (2002). Evaluating resource selection functions. *Ecological Modelling, 157*(2–3), 281–300. https://doi.org/10.1016/S0304-3800(02)00200-4

Cox, D. R. (1972). Regression models and life-tables. *Journal of the Royal Statistical Society: Series B, 34*(2), 187–220. https://doi.org/10.1111/j.2517-6161.1972.tb00899.x

Davidson-Pilon, C. (2019). lifelines: Survival analysis in Python. *Journal of Open Source Software, 4*(40), 1317. https://doi.org/10.21105/joss.01317

Diffendorfer, J. E., & Compton, R. W. (2014). Land cover and topography affect the land transformation caused by wind facilities. *PLoS ONE, 9*(2), e88914. https://doi.org/10.1371/journal.pone.0088914

Elliott, P., & Wartenberg, D. (2004). Spatial epidemiology: Current approaches and future challenges. *Environmental Health Perspectives, 112*(9), 998–1006. https://doi.org/10.1289/ehp.6735

European Environment Agency. (2019). *CORINE Land Cover 2018* [Data set]. https://land.copernicus.eu/en/land-cover

European Environment Agency. (2019). *Natura 2000 data — the European network of protected sites* [Data set]. https://www.eea.europa.eu/data-and-maps/data/natura-11

European Forest Fire Information System. (2024). *Burnt areas* [Data set]. Copernicus Emergency Management Service. https://forest-fire.emergency.copernicus.eu

European Space Agency, & Airbus. (2022). *Copernicus GLO-90 Digital Elevation Model* [Data set]. https://spacedata.copernicus.eu

Global Wind Atlas. (2023). *Mean wind speed at 100 m* [Data set]. Technical University of Denmark (DTU Wind Energy). https://globalwindatlas.info

Johnson, D. H. (1980). The comparison of usage and availability measurements for evaluating resource preference. *Ecology, 61*(1), 65–71. https://doi.org/10.2307/1937156

Manly, B. F. J., McDonald, L. L., Thomas, D. L., McDonald, T. L., & Erickson, W. P. (2002). *Resource selection by animals: Statistical design and analysis for field studies* (2nd ed.). Kluwer Academic Publishers.

Seabold, S., & Perktold, J. (2010). statsmodels: Econometric and statistical modeling with Python. *Proceedings of the 9th Python in Science Conference*, 92–96. https://doi.org/10.25080/Majora-92bf1922-011

Vlamakis, A., Eleftheriou, I., & Dima, S. (2025). *The real and unreal correlation between wind turbines and wildfires: Lessons from Greece* [Conference poster P122]. Celebrating Wind Conference (CWW) 2025, Montpellier, France.